Nothing has such power to broaden the mind as the ability to investigate systematically and truly all that comes under thy observation in life.

Marcus Aurelius Antoninius (121-180 AD)

Roman Emperor

Chapter 4

A RAMAN SPECTROSCOPIC STUDY OF THE EPICUTICULAR WAX LAYER OF MATURE MANGO (*Mangifera indica* L) FRUIT [1]

4.1 ABSTRACT

Raman spectroscopy was used to characterize the epicuticular wax of mature mango fruit. Little is known about the chemical composition of the natural wax layer covering mango (*Mangifera indica*) fruit. Scanning electron microscopy measurements showed two morphologically distinct parts in the wax layer and Raman microscopy determined that they are chemically distinct. Crystalline aliphatic compounds protrude from an amorphous layer in which long-chain aliphatic, aromatic and unsaturated compounds are present. Raman spectra recorded on the perimeter of lenticels indicate an absence of the crystalline aliphatic compounds in this region and this information could assist in the solution of a problem faced by the mango industry due to the discoloration around lenticels, which makes the fruit unacceptable as an export product. The results are supported by Fourier transform infrared spectroscopy. Both techniques are now employed as probes in a long-term project to study dynamic changes of the wax during fruit development and eventual processing. This includes the monitoring of possible changes in carotenoid content and the role of dust particles embedded in the wax.

4.2 INTRODUCTION

Mango (*Mangifera indica* L.) fruit, like most aerial parts of terrestrial plants, is covered by a thin wax layer, which as the outer boundary of the epicuticular layer, forms the interface

---

1: This chapter has been published as an article in the *Journal of Raman Spectroscopy* 35: 561 - 567.

between the plant and the atmosphere. It protects the fruit during growth against excessive exposure to UV radiation, plays a role as insect repellent, influences the uptake of foliar applied herbicides, and reduces water loss. It furthermore creates a water resistant surface, allowing dirt and pathogens to be washed away (Balsdon *et al*., 1995; Schwab *et al*., 1995; Barthlott & Neinhuis, 1997; Kirkwood, 1999). The mango skin is also characterised by the presence of lenticels, which are structures of epidermal origin with the function of gas exchange (O'Hare *et al*., 1999). These lenticels are present in large numbers and prone to discoloration that renders the fruit cosmetically unacceptable as an export product (Fig. 1). This leads to financial losses for South African mango industry. Furthermore, world trade in fresh mango fruit is restricted by the highly perishable nature of this fruit, which displays a characteristic peak of respiratory activity during ripening and is therefore considered to have a short storage life.

In order to control financial losses and fruit quality, control measures and improved long-term storage conditions must be employed to expand marketability of the fresh fruit (Jacobi *et al*., 2001). In South Africa, as part of postharvest treatments, the natural plant wax is mechanically altered during packline procedures, such as submersion of the fruit in hot water (± 48°C), which can cause heat injuries to the mango skin and influence fruit ripening (Jacobi *et al*., 2001). The wax is also chemically altered when a commercial wax, which prolongs the shelf life of the fruit by inhibiting water loss, is applied during packing. It is suspected though, that the interaction of the commercial wax with the natural wax can contribute to discoloration around lenticels, which is a manifestation of a physiological response to stress being imposed on the fruit.

Scanning electron microscopy (SEM) has been used extensively in previous studies to study the morphology of the wax layers, while gas chromatography coupled to mass spectroscopy (GC-MS) and high-performance liquid chromatography (HPLC) have been used to determine the chemical composition of plant wax. These studies have shown that the foremost components present in plant waxes are n-alkanes, alkyl esters, n-alkanoic acids, primary and secondary alcohols, aldehydes, mono- and diketones while free and esterified alcohols, and several fatty acids have been identified as some of the lesser components (Jetter, 2000; Kunst & Samuels, 2003).

Fourier transform infrared (FTIR) spectroscopy has been used to identify the presence of carbonyl groups in plant waxes and to study the phase behaviour and crystallinity of cuticular waxes (Merk *et al*., 1998; Dubis *et al*., 1999; Jetter & Riederer, 1999). Fourier transform-Raman spectroscopy was used in a study of the wax on Norwegian spruce

needles and identified carotenoids in micro and macro measurements (Matějka *et al*., 2001). Gas chromatography has also shown that the leaf epicuticular wax of *Prunus laurocerasus* L. occurs in a layered structure with different chemical compositions, which dynamically change during leaf development (Jetter *et al*., 2000; Jetter & Schäffer, 2001).

Raman and infrared microscopy were chosen in this study as possible methods to distinguish chemically between different wax fractions, which have been visually determined with Field Emission-SEM, as sampling size with the Raman microscope can be as small as 1 μm^2, and for the infrared microscope 20 μm^2. This makes it possible to distinguish between small fractions. A further advantage of the two methods is their ability to serve as non-destructive techniques, allowing the material to be isolated and investigated without any chemical change and interference during extraction procedures. We report here on the role of Raman and infrared microscopy in the preliminary part of the study.

In an attempt to understand and improve the postharvest performance of mangoes in general and the problem with lenticel discoloration in particular, this study was undertaken to characterise mango wax, compare it to the commercial wax and determine whether the interaction with commercial wax contributes to the discoloration effect. In so doing, it was necessary to examine the chemical composition and the morphology of the wax layers, since both of these factors contribute to the functional role of the wax.

4.3 MATERIAL AND METHODS

4.3.1 Plant material

Physiologically mature mango fruit were collected from an orchard in the Hoedspruit area, Limpopo Province, South Africa. They were carefully packed for transportation to the laboratory in order to prevent any damage to the fruit surface. Two different cultivars, namely ‘Keitt’ and ‘Tommy Atkins’, were investigated. Since the Raman and FTIR results for the two cultivars hardly differed, only the results for the cultivar ‘Keitt’ are presented.

4.3.2 Instrumentation

Raman spectra were recorded with a XY Raman spectrometer from Dilor, using the λ=514.5 nm laser line of a Coherent Innova 90 Ar^+-laser as exciting line. The spectra were recorded in a backscattering configuration with an Olympus microscope attached to the

instrument. The spectral resolution was at least 2 cm^{-1} for all the measurements. Optimum recording conditions were obtained by varying laser power, microscope objective and size of the confocal hole.

Mid-infrared transmission spectra were recorded of the same samples, using a Bruker infrared microscope (A 590), equipped with a MCT detector, attached to a Bruker 113v Fourier transform infrared (FTIR) spectrometer. The resolution was 4 cm^{-1} and 32 scans were signal-averaged in each interferogram. The 15x objective was used in all instances with a sample aperture size of 80 μm^2.

Powder X-ray diffraction data from soil samples collected in the mango orchard was recorded with a Siemens D501 automated diffractometer equipped with a secondary graphite monochromator. The applied potential was 40 kV and the corresponding current 40 mA. Cu Kα-radiation was used as the primary X-ray beam. A pattern was recorded from 3 to 70° (2θ) in steps of 0.05°. The measuring time was 1 s and the scanning speed 3° (2θ) per minute.

Electron micrographs were obtained using a JSM-6000F scanning electron microscope (JEOL, Tokyo, Japan). The samples were plunge frozen in liquid propane at -180 °C and vacuum dried in a Fisons E6441 High Vacuum Evaporation Unit (Fisons, East Sussex, England) for 72 hours. They were made conductive by exposing it to 0.5 % RuO_4 vapour for 30 minutes (Van der Merwe & Peacock, 1999).

4.4 RESULTS AND DISCUSSION

4.4.1 Microscopic characterisation of mango fruit wax

The cuticle of physiological mature fruit (cv. 'Keitt') is covered with a distinctive layer of wax in which two different regions can be distinguished (Fig. 2). The outermost layer consists of microscopic wax crystaloids (Fig. 2A) that form an irregular surface and protrude from an amorphous wax film underneath (Fig. 2B). Such morphological distinctiveness is due to differences in the chemical composition of the various components contributing to each fraction (Griffiths *et al*., 1999; Griffiths *et al*., 2000; Jetter *et al*., 2000).

4.4.2 *In vivo* measurements

In the first experiments, Raman spectra were recorded *in vivo* on small pieces of mango rind from which the pulp had been removed. It was hoped that the confocal Dilor XY system would make it possible to differentiate between wax layers in the z-direction by changing the depth of focus. However, a strong fluorescence background, which was stronger on the yellow part of the rind than on the green, made it difficult to obtain useable spectra. Decreasing the laser power to 0.5 mW at the sample and using the 50x objective of the microscope reduced the fluorescence sufficiently to obtain the baseline corrected spectrum shown in figure 3. Spectra recorded on the green and yellow parts of the rind respectively were identical and are typical of carotenoid pigments, which occur in many fruit and vegetables. Carotenoid pigments play an important role in photosynthesis as they protect the photosynthetic system from photo-oxidative damage and are accessory light-harvesting pigments, as they absorb light in wavelength regions where the chlorophylls absorb weakly. Raman and resonance Raman spectroscopy have been used extensively to study the molecular structure and configuration of the carotenoid molecules that occur in light-harvesting proteins and reaction centres (Robert, 1999; Ruban *et al*., 2000; Ruban *et al*., 2001).

Carotenoids are very efficient Raman scatterers and most exhibit a resonance or pre-resonance enhancement due to the 514.5 nm laser exciting line. Consequently, any bands that may originate from the wax are dwarfed by the spectrum of the pigment underneath the wax layer. The most intense peaks in the carotenoid spectrum occur at 1524 cm^{-1} (ν_1, -C=C- stretching vibrations), 1156 cm^{-1} (ν_2, -C-C- stretching) and 1005 cm^{-1} (ν_3, $-CH_3$ in-plane rocking vibrations) (Robert, 1999; Ruban *et al*., 2000; Ruban *et al*., 2001; Withnall *et al*., 2003). The ν_4 band at 964 cm^{-1} is attributed to out-of-plane C-H modes, which are formally forbidden for planar molecules, but when carotenoid molecules are twisted around a C-C bond these out-of-plane modes become more strongly coupled to the electronic transitions and their contributions to the resonance Raman spectra become more intense. Bands in this region have proved useful to identify carotenoids in biological samples using different resonance conditions (Ruban *et al*., 2001).

The peak position of the ν_1 band in the Raman spectrum is determined by the number of conjugated double bonds in the molecule, which also determines the colour, ranging from yellow to purple, of carotenoid pigments. The position of the band shifts to higher wavenumbers for *cis*-isomers and the presence of more than one carotenoid, with different resonance effects in biological samples influences the position of the band

(Robert, 1999; Ruban *et al*., 2000; Ruban *et al*., 2001; Withnall *et al*., 2003). It is therefore not always easy to identify carotenoids using the ν_1 value and a spectrum from a carrot slice with known carotenoid content (90 % β-carotene, 10 % α-carotene), was recorded with the same experimental conditions used for the mango measurements, to use as reference. The ν_1 value obtained for the carrot slice at 1519 cm^{-1} is similar to that obtained by Withnall *et al*. (2003) (514.5 nm exciting line) and is 5 cm^{-1} lower than the value of 1524 cm^{-1} of mango fruit rind. Recent studies have identified all-*trans*-β-carotene, all-*trans*-violaxanthin and 9-*cis*-violaxanthin as the major carotenoids present in mango fruit (Rodriguez-Amaya, 2000; Pott *et al*., 2003). It has been determined that the ν_1 value for violaxanthin occurs at 1528 cm^{-1} with 514.5 nm excitation. Thus the upwards shift of the ν_1 band in the carrot spectrum at 1519 cm^{-1}, with only α-carotene and β-carotene present, to 1524 cm^{-1} in the mango spectrum is probably caused by the contribution of both isomers of violaxanthin.

4.4.3 Freeze-dried samples

The rind from the mature fruit, which was plunge-frozen and freeze-dried for SEM studies gave the same fluorescence problem experienced with the fresh fruit and could not be used to obtain spectra from the surface wax.

In order to eliminate the strong resonance enhanced signal from the β-carotene and the fluorescence background, subsequent wax samples were then manually removed from the mango surface with a surgical scalpel and placed on microscope slides. This was done in progressive layers in order to make it possible to differentiate between the top and bottom layers of the wax (Fig. 2 A & B).

4.4.4 Outermost wax layer

The Raman and infrared spectra of waxes may be considered in two wavenumber regions, namely: 600-1800 cm^{-1}, which contains functional groups, as well as information about skeletal backbone vibrations, and 2700-3600 cm^{-1}, which is dominated by C-H, N-H and O-H stretching bands.

Three Raman spectra (Fig. 4), recorded from different parts of the fruit epicuticular wax layer, are shown in the region 1000-1700 cm^{-1}. The simplicity of the spectrum of the uppermost wax layer (Fig. 4 A; Table 1) is typical of long-chain aliphatic compounds, with the very strong band at 1295 cm^{-1}, representing $-(CH_2)_n-$ twisting vibrations, the most prominent band in this region. The main peak of the bending vibrations of the CH_2 moiety

is observed at 1439 cm^{-1} and a weak wagging vibration at 1370 cm^{-1} (Lin-Vien *et al*., 1991; Cao *et al*., 1995; Schrader, 1995; Coates, 2000).

In the region between 1000 and 1100 cm^{-1} various bands representing C-C stretch vibrations occur and the two sharp bands at 1161 and 1130 cm^{-1} have been assigned to all-trans chain segments (Cao *et al*., 1995).

The infrared spectrum of the same region is shown in Figure 5 and the in-phase rocking mode at 719 cm^{-1} confirms that the wax is an alkane with n>4. On closer examination it is seen that both the $-(CH_2)_n-$ scissoring mode (1462-, 1472 cm^{-1}) and in phase rocking mode (719-, 729 cm^{-1}) are split. This is similar to the values for polyethylene and is ascribed to factor-group splitting because of interaction between molecules in orthorhombic crystalline areas (Coates, 2000). The strong band in the infrared spectrum at 1709 cm^{-1}, is assigned to a C=O vibration and confirms the presence of long-chain aliphatic ketone or fatty acid (Dubis *et al*., 1999). Lack of coincidence of Raman and infrared bands in the spectra are typical of polyethylene type of compounds, where a local centre of symmetry exists in the middle of $-CH_2{-}CH_2-$ groups, making the rule of mutual exclusion active (Schrader, 1995).

The stretching vibrational modes of CH_2- and CH_3- groups occur in the region 2700-3600 cm^{-1}. In Figure 6 A the bands in this region of the outermost wax layer is shown and is dominated by the symmetric (in-phase) and anti-symmetric (out-of-phase) stretching vibrations of the methylene chain at 2846 and 2881 cm^{-1} respectively. Smaller peaks at 2904 and 2930 cm^{-1} are attributed to motions of terminal CH_3 groups. The peak-height intensity ratio I_{2846}/I_{2881} is very sensitive to chain packing and has been used to determine inter-chain interactions, whilst I_{2930}/I_{2881} measures effects from intra-chain interactions (Levin & Lewis, 1990). The spectra in this region were deconvoluted with the Labspec software supplied with the Dilor Raman instrument and it was found that I_{2846}/I_{2881} = 0.8 and I_{2930}/I_{2881} = 0.05 for the aliphatic layer. The high value of I_{2846}/I_{2881} is an indication of an ordered system and therefore high crystallinity, with little interaction between the chains, which is supported by the low value of I_{2930}/I_{2881}. The infrared spectrum of this layer (Table 1) exhibited the strong symmetric and asymmetric CH_2 stretch vibrations at 2848 cm^{-1} and 2918 cm^{-1} respectively.

4.4.5 Wax layer adjacent to the cuticle

The Raman and FTIR spectra have identified the wax crystals, seen on the outer boundary (Fig. 2 A), as long-chain alkanes, most probably ketones or fatty acids. The

Raman and FTIR spectra of the layer adjacent to the cuticular layer display the same bands mentioned above (Fig. 2 B), but also exhibit new bands in the 600-1800 cm^{-1} region at 1607 and 1632 cm^{-1}. The band at 1607 cm^{-1} is very typical of the conjugated C-C vibrations of aromatic rings, while the band at 1632 cm^{-1} occurs at a position usually associated with isolated C=C vibrations (Coates, 2000). Evidently the two wax layers are chemically distinct, with crystalline long-chain aliphatic compounds the main constituents of the outermost layer, whilst the layer beneath is a mixture of aliphatic, aromatic and unsaturated compounds. In the infrared spectrum of this layer a new band has appeared in the C=O stretching region at 1734 cm^{-1}, which could be an indication of the presence of esters in this wax fraction (Dubis *et al*., 1999).

In figure 6 B the Raman spectrum of this layer is shown in the region of the C-H stretch vibrations. The two bands at 2846 and 2881 cm^{-1} have slightly shifted towards higher wavenumbers namely 2850 and 2883 cm^{-1} respectively, which suggests that the disorder of the chains has increased (Cao *et al*., 1995). The amount of methyl groups has increased as the small bands observed as shoulders at 2904 and 2930 cm^{-1} due to stretch vibrations of CH_3 -groups are more intense. The ratio I_{2850}/I_{2883} decreased from 0.8 in the top layer to 0.7 and the ratio I_{2935}/I_{2883} increased from 0.1 for the top layer to 0.4 in the layer containing the aromatic compounds. This is an indication of a decrease in crystallinity and an increase in inter-chain interactions, which would imply a more disordered amorphous structure. The infrared bands in this region have previously been used to study the temperature related phase behaviour of plant wax (leaves from *Hedera helix* L. and *Juglans regia* L.) (Merk *et al*., 1998), but we did not observe the same sensitivity to phase as with our Raman measurements in this region and therefore only used the Raman data to determine qualitatively, crystallinity.

4.4.6 Analysis of wax around the lenticels

Raman spectra of the wax covering the area surrounding a lenticel were obtained in vivo on samples where the fruit rind had been carefully removed from the lenticel, but with the basic structure still intact. One of these spectra can be seen in Figure 2 C and it is clear that the peaks ascribed to the aliphatic long-chain compounds have disappeared almost completely as best illustrated by the dramatic decrease in intensity of the $-(CH_2)_n-$ twisting mode at 1295 cm^{-1}. The C=C stretch peaks around 1600 cm^{-1} are now the most dominant peaks in the spectrum. The ratio indicating crystallinity, I_{2850}/I_{2883} =0.8 is similar to that of the amorphous layer, but the ratio I_{2930}/I_{2883} increased from 0.4 in the aromatic/aliphatic layer to 0.7, which indicates more inter-chain interaction as well as the presence of more $-CH_3$ end-groups. The absence of the nematoid crystals, consisting of long-chain aliphatic

compounds, around the lenticels is visually confirmed in Figure 7. The chemical and physical characteristics of the wax covering around lenticels are clearly different from the surroundings and postharvest treatments of the mango might affect this area differently than the rest of the rind.

4.4.7 Analysis of industrial wax

Raman spectra of the industrial wax used to cover mangoes in South Africa could not be obtained due to fluorescence. The FTIR spectrum of unblended Carnauba wax, derived from the leaves of Carnauba palms and commonly used as commercial wax, is shown in Figure 8. It is clear that the spectrum is very similar to that of the mango wax, but the splitting of the bands at 720 and 1470 cm^{-1} (indicative of crystallinity and a high degree of regularity for the backbone structure) observed in both fractions of mango wax, is not present. The FTIR spectra of two other commercial products namely Mangoshine® and Biocote® did show this splitting and therefore consists of more crystalline fractions than unblended Carnauba wax. One of the aims of the long-term project would be to establish if there is a difference in performance of the different commercial waxes and if the presence of a crystalline fraction in the commercial waxes prevents or contributes to lenticel damage.

4.4.8 Dust particles on mango surface

Small crystallites were observed between the wax crystals during the in vivo Raman measurements. The 100x objective of the Raman microscope made it possible to record spectra of these crystals individually and the results are presented in Figure 9. In the uppermost spectrum (Fig. 9 A) the most prominent peak at 462 cm^{-1} clearly indicates the presence of α-quartz in a reddish crystallite and the two smaller peaks at 219 and 290 cm^{-1} belong to Fe_2O_3, which is present in small quantities in most South African soils and responsible for the reddish colour of the α-quartz (Gillet, 2002). The middle spectrum (Fig. 9 B) with peaks at 290, 475 and 506 cm^{-1} resembles the spectrum of feldspar (albite form) and the bottom spectrum (Fig. 3 C) is assigned to TiO_2 with the very intense peak at 143 cm^{-1} and peaks at 396 cm^{-1}, 514 cm^{-1} and 640 cm^{-1} characteristic of the anastase phase. It can be deducted that this outermost wax layer, with its microscopically rough surface, entraps ultra-fine dust particles from the surroundings and in this way protects against penetration to the inner layer and the fruit itself. X-ray powder diffraction (XRD) data confirmed that dust collected in the vicinity of the mango trees used in this study were a mixture of mainly α-quartz and feldspar in the albite form ($NaAlSi_3O_8$), with small percentages of muscovite, orthoclase, sepiolite and kaolinite present. The spectrum of

TiO_2 was not obtained on a crystallite, but on the wax itself as can be seen by the presence of the characteristic peaks of the aliphatic wax layer in the spectrum. However, since this was the only instance in which the particular spectrum was obtained, it too is suspected to be contamination and not an intrinsic part of mango wax. Although TiO_2 was also not detected with XRD, it is present as a trace compound in many South African soils and the very strong Raman bands make small quantities easy to detect.

4.5 CONCLUSION

Epicuticular waxes are complex mixtures that consist of a great number of components, which vary greatly between plant species. Many of these constituents have very similar Raman and infrared spectra and differ structurally only in chain-length and a functional group or two. It is thus impossible to identify all the components of the wax using Raman spectroscopy alone, but we have shown that Raman spectroscopy could chemically distinguish between morphologically different wax fractions as observed with SEM measurements and that FTIR measurements fulfil a complimentary role in the identification of some functional groups.

It has previously been shown that the morphology and chemical composition of the epicuticular wax changes dynamically during the growth of mango fruit (Bally, 1999). In the forthcoming mango season, Raman microscopy will be linked the morphological changes to chemical changes in the wax layer that occur during fruit ripening and so elucidate the biosynthetic pathways of the wax formation.

The enhancement of the Raman signal of most carotenoid pigments with the 514.5 nm line makes Raman microscopy also a useful tool to study pigment distribution and formation during mango fruit development. In the long term project, the use of different laser lines is envisaged to help in the identification of different carotenoid pigments, as well as the possible enhancement of chlorophyll bands to study the modification of both pigments during the growth and ripening processes. The pigmentation around lenticels will be of special interest, and in combination with fluorescence microscopy and HPLC will contribute to a better understanding of the discoloration problem.

The microscopic identification of dust particles on the wax surface makes it possible to study the influence of external factors, which may be harmful. At this stage, it is not clear if the dust particles play any role in the discoloration around lenticels, but the amount and

presence of the particles shall be monitored. The detection of such small quantities of foreign matter holds particularly useful potential in the surveillance of pre-harvest control measures such as the detection of fungicidal copper compounds.

A better understanding of the chemistry and morphology of the wax surface can contribute to the improvement of postharvest treatments, which could lead to financial benefits for the mango industry.

4.6 REFERENCES

Bally, I.S.E. 1999. Changes in the cuticular surface during the development of mango (*Mangifera indica* L.) cv. Kensington Pride. *Scientia Hort*.: 79: 13 - 22.

Balsdon, J.A., Espelie, K.E. & Braman, S.K. 1995. Epicuticular lipids from azalea (*Rhododendron* spp.) and their potential role in host plant acceptance by azalea lace bug, *Stephanitis pyrioides* (Heteroptera: Tingidae). *Biochem. Syst. Ecol*. 23 (5): 477 - 485.

Barthlott W. & Neinhuis, C. 1997. Purity of the sacred lotus, or escape from contamination in biological surfaces. *Planta* 202: 1 - 8.

Cao, A., Liquier, J. & Taillandier, E. 1995. *Infrared and Raman spectroscopy of biomolecules. Methods and Applications*, pp. 344 - 363. (Ed.) Schrader, B. John Wiley & Sons Ltd., London, UK.

Coates, J. 2000. Interpretation of Infrared Spectra: A Practical Approach. In*: Encyclopedia of Analytical Chemistry*, pp. 10815 - 10837. (Ed.) Meyers, R.A. John Wiley & Sons Ltd., Chichester, UK.

Dubis, E.N., Dubis, A.T. & Morzyki, J.W. 1999. Comparative analysis of plant cuticular waxes using HATR FT-IR reflection technique. *J. Mol. Struct*. 511-512: 173 - 179.

Gillet, P. 2002. Applications of Vibrational Spectroscopy to Geology. In: *The Handbook of Vibrational Spectroscopy IV,* pp. 75 - 103. John Wiley & Sons Ltd., London.

Griffiths, D.W., Robertson, G.W., Shepherd, T. & Ramsay, G. 1999. Epicuticular waxes and volatiles from faba bean (*Vicia faba*) flowers. *Phytochem.* 52: 607 - 612.

Griffiths, D.W., Robertson, G.W., Shepherd, T. & Ramsay, G. 2000. A comparison of the composition of epicuticular wax from red raspberry (*Rubus idaesus* L.) and hawthorn (*Crateagus monogyna* Jacq.) flowers. *Phytochem.* 55: 111 - 116.

Jacobi, K.K., Macrae, E.A. & Hetherington, S.E. 2001. Postharvest heat disinfestation treatments of mango fruit. *Scientia Hort*. 89: 171 - 193

Jetter, R. & Riederer, M. 1999. Homologous long-chain d-lactones in leaf cuticular waxes of *Cerinthe minor*. *Phytochem*. 50: 1359 - 1364.

Jetter, R. 2000. Long-chain alkanediols from *Myricaria germanica* leaf cuticular waxes. *Phytochem*. 55: 169 - 176.

Jetter, R., Schäffer, S. & Riederer, M. 2000. Leaf cuticular waxes are arranged in chemically and mechanically distinct layers: evidence from *Prunus laurocerasus* L. *Plant Cell Environ*. 23: 619 - 628.

Jetter, R. & Schäffer, S. 2001. Chemical composition of the *Prunus laurocerasus* leaf surface. Dynamic Changes of the epicuticular wax film during leaf development. *Plant Physiol*. 126: 1725 - 1737.

Kirkwood, R.C. 1999. Recent developments in our understanding of the plant cuticle as a barrier to the foliar uptake of pesticides. *Pest. Sci*. 55: 69 - 77.

Kunst, L. & Samuels, A.L. 2003. Biosynthesis and secretion of plant cuticular wax. *Prog. Lipid Res*. 42: 51 - 80.

Levin, I.W. & Lewis, E.N. 1990. Fourier transform Raman spectroscopy of biological materials. *Anal. Chem*. 62 (21): 1101A - 1111A.

Lin-Vien, D., Colthup, N.B., Fateley, W.G. & Graselli, J.G. 1991. *The Handbook of Infrared and Raman Characteristic Frequencies of Organic Molecules*, pp. 1 - 73. Academic Press. Inc., Harcourt Brace Jovanovich Publishers, San Diego.

Matějka, P., Plešerová, L., Budínová, G., Havířová, K., Mulet, X., Skácel, F. & Volka, K. 2001. Vibrational biospectroscopy: What can we say about the surface wax layer of Norway spruce needles? *J. Mol. Struct.* 566: 305 - 310.

Merk, S., Blume, A. & Riederer, M. 1998. Phase behaviour and crystallinity of plant cuticular waxes studied by Fourier transform infrared spectroscopy. *Planta* 204: 44 - 53.

O'Hare, T.J., Bally, I.S.E., Dahler, J.M., Saks, Y. & Underhill, S.J.R. 1999. Characterisation and induction of 'etch' browning in the skin of mango fruit. *Postharvest Biol. Technol*. 16: 269 - 277.

Pott, I., Breithaupt, D.E. & Carle, R. 2003. Detection of unusual carotenoid esters in fresh mango (*Mangifera indica* L. cv. 'Kent'). *Phytochem*. 64: 825 - 829.

Robert, B. 1999. The electronic structure, stereochemistry and resonance Raman spectroscopy of carotenoids. In: *The Photochemistry of Carotenoids*, pp. 189 - 201. (Eds.) Frank, H.A., Young, A.J., Britton, G. & Cogdell, R.J. Kluwer, Dordrecht, The Netherlands.

Rodriguez-Amaya, D.B. 2000. Some considerations in generating carotenoid data for food composition tables. *J. Food Compos. Anal*. 13: 641 - 647.

Ruban, A.V., Pascal, A.A. & Robert, B. 2000. Xanthophylls of the major photosynthetic light-harvesting complex of plants: identification, conformation and dynamics. *FEBS Lett.* 477 (3): 181 - 185.

Ruban, A.V., Pascal, A.A., Robert, B. & Horton, P. 2001. Configuration and dynamics of carotenoids in light-harvesting antennae of the thylakoid membrane. *J. Biol. Chem*. 276 (27): 24862 - 24870.

Schrader, B. 1995. *Organic substances. Infrared and Raman Spectroscopy - Methods and Applications*, pp. 63 - 162. (Ed.) Schrader, B. John Wiley & Sons Ltd., London, UK.

Schwab, M., Noga, G. & Barthlott, W. 1995. The significance of cuticular wax among *Salix* species and *Populus* species hybrids. *Gartenbauwiss*. 60 (3): 102 - 109.

Van der Merwe, C.F. & Peacock, J. 1999. Enhancing conductivity in biological material for SEM. *Proc. Microsc. Soc. south. Afr*. 29: 44.

Withnall, R., Chowdhry, B.Z., Silver, J., Edwards, H.G.M. & De Oliveira, L.F.C. 2003. Raman spectra of carotenoids in natural products. *Spectrochim. Acta A* 59: 2207 - 2212.

4.7 TABLES

Table 1 Wavenumbers (in cm^{-1}) and assignment of main Raman and infrared bands of crystalline and amorphous wax fractions

Aliphatic layer[a]	Aromatic/unsaturated[a]	Assignment
719 (s) IR 729 (s) IR	719 (m) IR 729 (m) IR	$-CH_2-$ rocking, $n > 3$
1036 (w) IR		C–C stretch
1107 (w) IR	1105 (w) IR	C–C stretch
1061 (m) R		C–C stretch
1130 (m) R		C–C stretch
1170 (w) R	1170 (m) R 1169 (sm) IR	Ring in-plane CH deformation
1295 (s) R		$-CH_2-$ twisting
1300 (w) IR		
1416 (m) R		CH_2 wagging
1439 (m) R	1462 (br) R	Anti-sym. CH_3 bending
1462 (m) IR 1471 (m) IR	1462 (m) IR	CH_2 scissoring
1586 (m) R		C=C stretch
1607 (s) R		Aromatic C=C stretch
1632 (m) R		Unsaturated C=C stretch
1709 (s) IR	1709 (s) IR	C=O stretch
1734 (s) IR	C=O stretch	
2846 (vs) R, 2848 (vs) IR	2850 (s) R, 2848 (s) IR	CH_2 symmetric stretch
2881 (vs) R, 2917 (vs) IR	2883 (s) R, 2918 (s) IR	CH_2 asymmetric stretch
2902 (w, sh) R	2902 (m) R	CH_3 stretch
2930 (w, sh) R	2930 (m) R	CH_3 stretch

[a] s = Strong; m = medium; w = weak; v = very; br = broad; sh = shoulder; R = Raman; IR = infrared

4.8 FIGURE CAPTIONS

Figure 1 Mango fruit with lenticel damage

Figure 2 Image of mango wax showing two distinct wax layers A) and B) and the cuticle C)

Figure 3 Spectrum of carotenoid pigment, recorded in vivo on mango fruit rind.

Figure 4 Raman spectra of mango wax of different parts of the wax: A) crystalline outermost layer, B) smooth layer next to cutin and C) area around lenticel.

Figure 5 Infrared spectra of mango wax: A) crystalline outermost layer and B) layer adjacent to cutin.

Figure 6 Raman spectra of mango wax in the region of the C-H stretch vibrations: A) outermost wax layer B) layer next to cutin and C) area round lenticel.

Figure 7 Micrograph of epicuticular surface around lenticel.

Figure 8 FT-IR spectrum of Carnauba wax.

Figure 9 Raman spectra of inorganic compounds recorded on mango wax A) Fe_2O_3 and α-quartz B) feldspar and C) TiO_2 (anastase) together with aliphatic wax layer.

4.9 FIGURES

Figure1

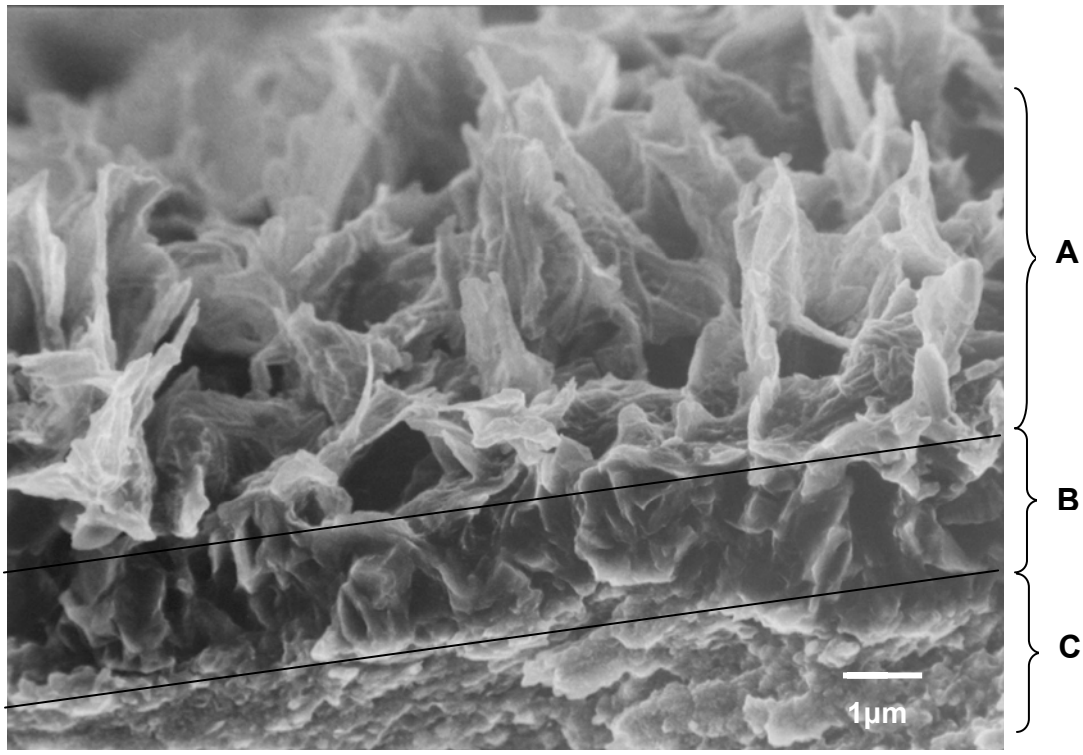

Figure 2

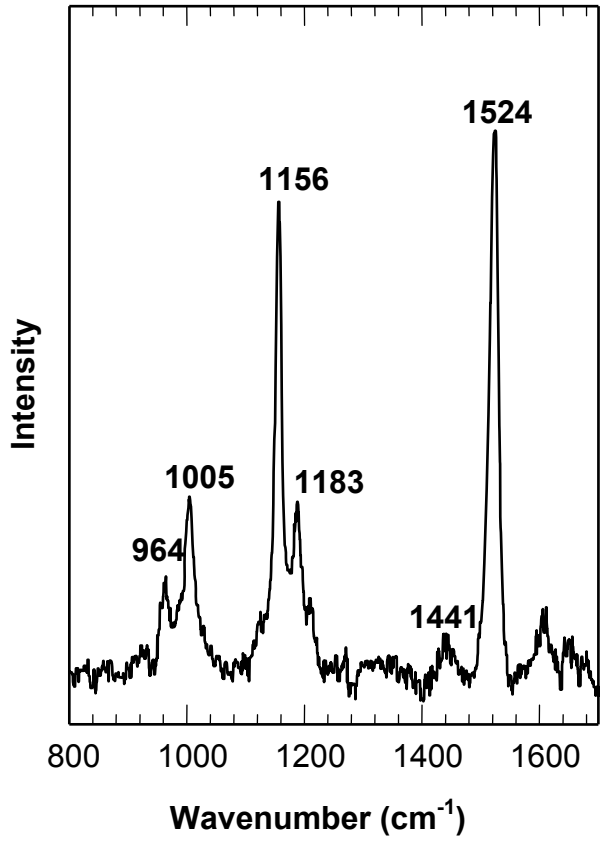

Figure 3

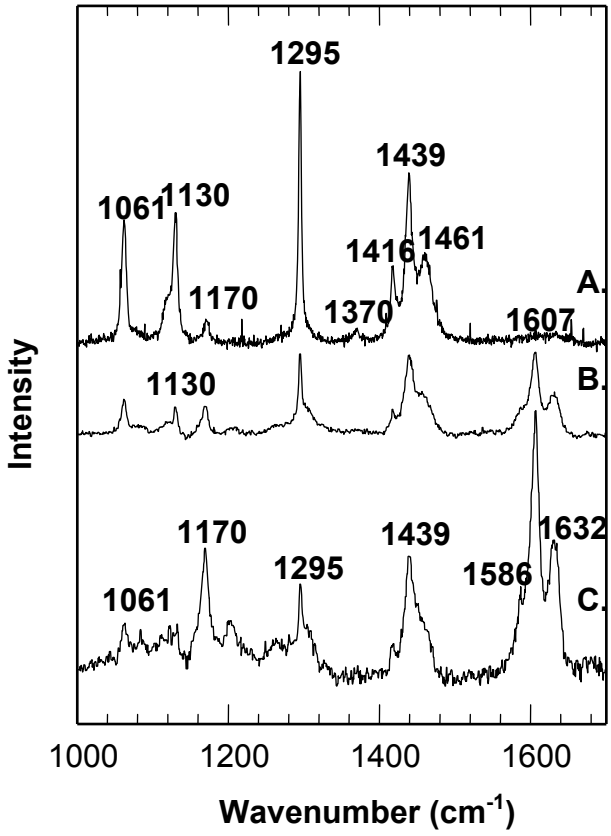

Figure 4

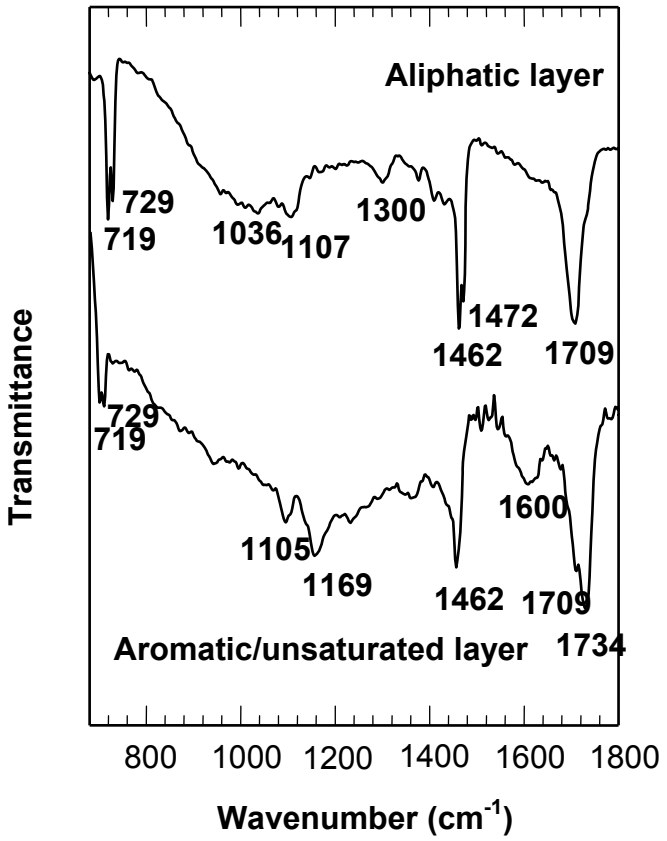

Figure 5

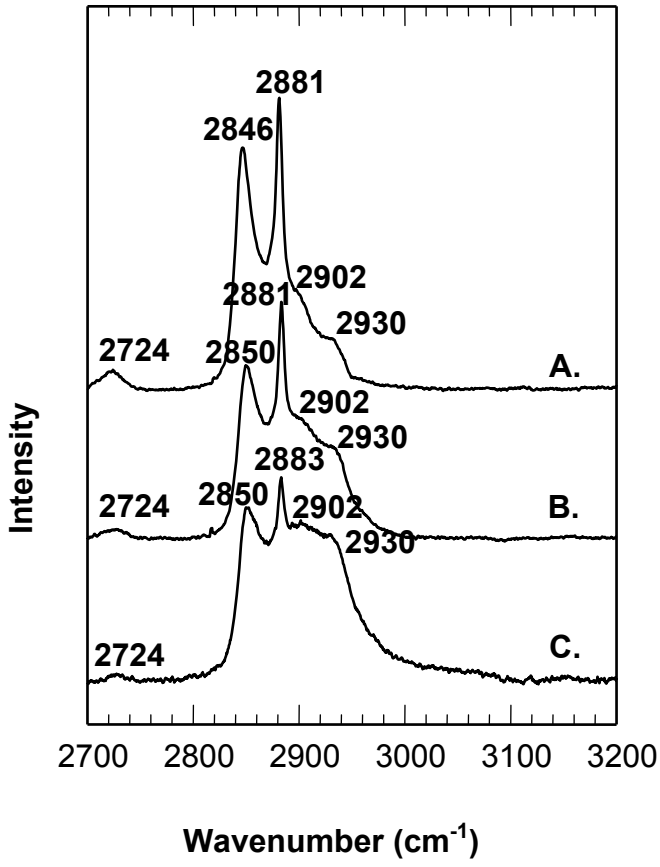

Figure 6

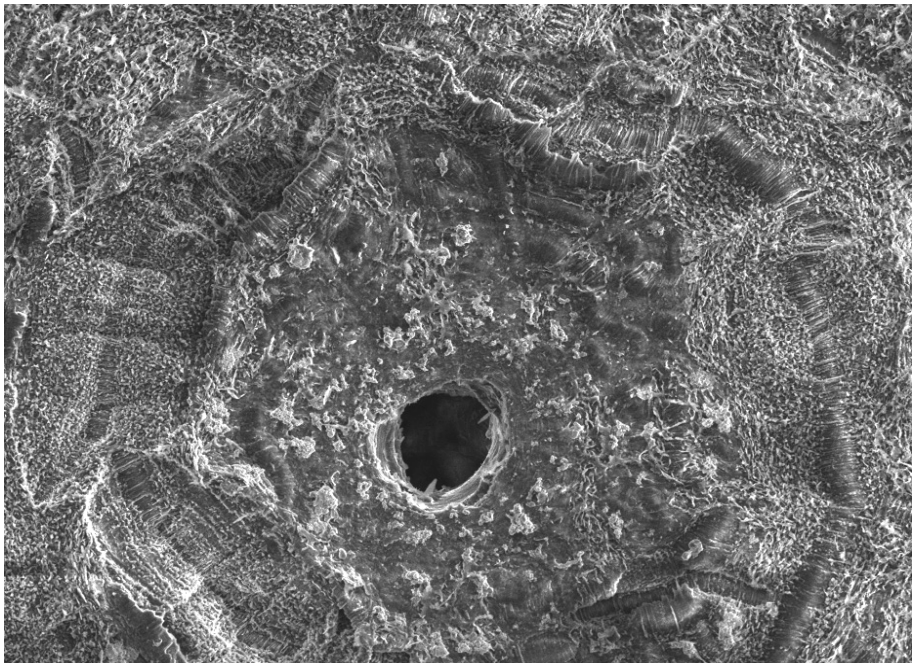

Figure 7

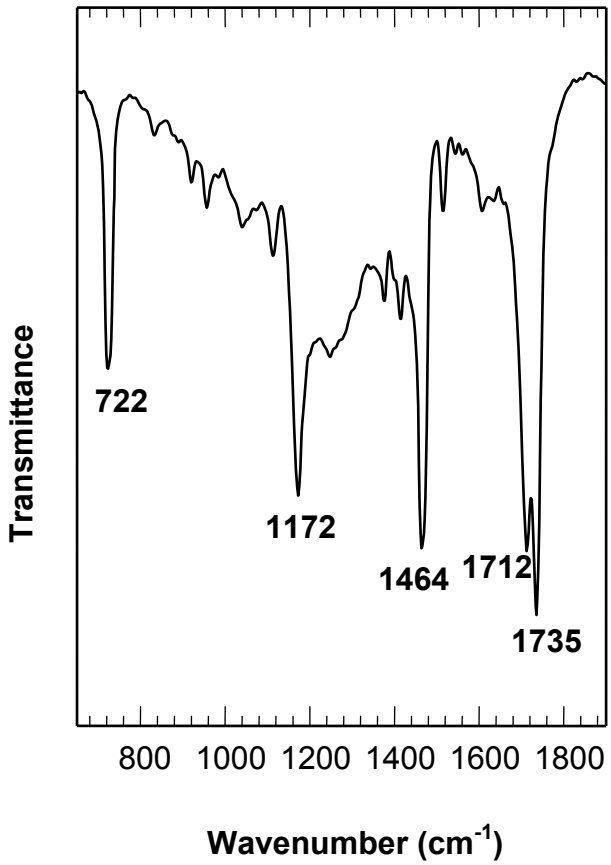

Figure 8

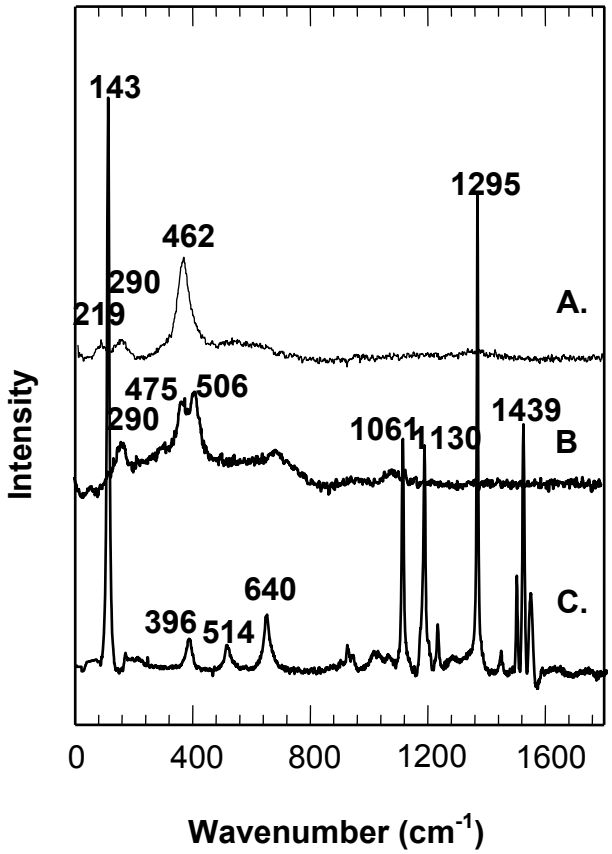
143
1295
462
290
219
A.
475
506
290
1061
1130
1439
B
640
396
514
C.
Intensity
0
400
800
1200
1600
Wavenumber (cm-1)

Figure 9